Electronic Supplementary Material (ESI) for Organic Chemistry Frontiers.

21-Carba-23-oxaporphyrinoids and 21-Oxo-21-carba-23-oxaporphyrinoids – Macrocyclic π-Conjugation Involving Carbonyl Moiety

Anna Berlicka*, Paulina Foryś-Martowłos, Karolina Hassa, Michał J. Białek, Katarzyna Ślepokura, and Lechosław Latos-Grażyński*

Supporting Information

Table of Contents

Experimental Procedures **2**

NMR spectroscopy 2
Mass spectrometry 2
Electronic spectroscopy 2
DFT calculations 2
X-ray data 2
Synthetic procedures and analytical data 4

Results and Discussions **10**

Schemes 10
X-ray structures 11
^{1}H NMR spectra 12
^{13}C NMR spectra 16
2D NMR spectra 19
UV-vis spectra 20
DFT figures and tables 23
References **25**

Experimental Procedures

NMR Spectroscopy

NMR spectra were recorded on Bruker Avance 500 MHz and Bruker Avance III 600 MHz spectrometers. Spectra were referenced to the residual solvent signal ($CDCl_3$, 7.24 and 77.0 ppm; CD_2Cl_2, 5.32 and 54.0 ppm). Two dimensional NMR spectra were recorded with 2048 data points in the t_2 domain and up to 1024 points in the t_1 domain, with a 1s recovery delay. ^{13}C NMR spectra of 21-carba-23-oxaporphyrins **14**, **14a** and 21-carba-23-oxachlorins **15**,**15a** were measured for their monoprotonated forms because of possible tautomerization shown in Schemes S2 and S3.

Mass Spectrometry

Mass spectra (High Resolution and Accurate Mass) were recorded on Bruker micrOTOF-Q, Shimadzu Q-TOF LCMS 9030 and WATERS LCT Premier XE spectrometers using the electrospray ionization technique.

UV/Vis Spectroscopy

Electronic spectra were recorded in CH_2Cl_2 solutions on a Varian Carry-50 Bio spectrophotometer.

DFT calculations

Geometry optimizations were carried out within unconstrained C_1 symmetry in vacuo, with starting coordinates derived from preoptimized models or crystal structures using Gaussian software.[1] Harmonic frequencies were calculated using analytical second derivatives to verify local minimum achievement with no negative frequencies observed. The calculations were performed at B3LYP/6-31G(d,p) level of theory.[2,3] NICS values[4] and NMR shifts were calculated using the GIAO method with TMS shieldings as a reference for NMR. For relative energy calculations, values with zero-point correction were taken. AICD plots were obtained by generation of the input file from CSGT calculations (Gaussian 09) and its processing by the AICD program.[5]

X-ray data for 14·xC_6H_{14} and 15a·0.5CH_2Cl_2

X-ray quality crystals of **14**·xC_6H_{14} and **15a**·0.5CH_2Cl_2 were both prepared by slow diffusion of hexane to solutions of **14** and **15** dissolved in dichloromethane. X-ray diffraction data for the crystals were collected at 100(2) K on a κ-geometry Rigaku XtaLAB Synergy DW (with rotating anode) or an Agilent Technologies Gemini Ultra four-circle diffractometer (ω scans) with Cu$K\alpha$ radiation. Data collections, cell refinements, data reductions and analyses, including analytical or empirical (multi-scan) absorption corrections, were carried out with *CrysAlisPRO*.[6] Structures were solved using dual-space algorithm with *SHELXT* program[7] and refined on F^2 by a full-matrix least-squares technique using *SHELXL-2014* program[8] with anisotropic displacement parameters for all non-H atoms.

There is a half of **14** molecule in the asymmetric unit of the **14**·xC_6H_{14} crystal (Z' = 0.5) and two molecules of **15a** and one CH_2Cl_2 molecule in the asymmetric unit of **15a**·0.5CH_2Cl_2 (Z' = 2). In **14**·xC_6H_{14} highly disordered solvent molecule (most probably *n*-hexane from crystallization solution) was detected. It was not modelled and their electron density was taken into account using the SQUEEZE procedure[9] in *PLATON* program.[10] Disordered *n*-hexane molecules are located in the hydrophobic channels running down the **c** axis. The volume of the solvent accessible voids (473 Å^3 and 123 electrons per unit cell, i.e. about 118 Å^3 and 31 electrons per molecule of **14**) suggests that the chemical formula of the crystal might be **14**·0.5C_6H_{14}.

p-Tolyl ring in **14**·xC_6H_{14} was found to be disordered and was refined in two positions with site occupation factors of 0.613(7) and 0.387(7). To get acceptable and appropriate model of this disordered fragment, some constraints on the coordinates and displacement parameters (EXYZ and EADP instructions in *SHELXL*) as well as restraint on the U_{ij} (ISOR) were applied in the refinement procedure.

All H atoms (including both positions of those from NH groups) in **14**·xC_6H_{14} and **15a**·0.5CH_2Cl_2 were found in difference Fourier maps. N-bound H atom in **14**·xC_6H_{14} (s.o.f. = 0.5) was refined freely. N-bound H atoms in **15a**·0.5CH_2Cl_2 (two positions of one H atom per molecule) were initially refined freely with isotropic displacement parameters and site occupation factor (s.o.f.) 0.5, resulting in a rational model (with the correct geometry, i.e. N–H distances, C–N–H angles and U_{iso} for H atoms). In the final refinement cycles, all the H atoms in **15a**·0.5CH_2Cl_2 and C-bound H atoms in **14**·xC_6H_{14} were repositioned in their calculated positions and refined using a riding model, with N–H = 0.88 and C–H = 0.95–0.99 Å, with U_{iso}(H) = 1.2U_{eq}(N,C) for NH, CH and CH_2 or U_{iso}(H) = 1.5U_{eq}(C) for CH_3, and with s.o.fs. of the NH hydrogen atoms = 0.5.

The details of structures refinements are given in Table S1. The crystallographic information files (CIF) have been deposited at the Cambridge Crystallographic Data Centre (CCDC Nos. **2177053, 2177054**) and provided as Supporting Information.

Table S1. Crystal data for **15a**·0.5CH_2Cl_2 and **14**·xC_6H_{14}.

	14·xC_6H_{14} [(a)]	**15a**·0.5CH_2Cl_2
CCDC No.	2177053	2177054
Chemical formula	$C_{35}H_{26}N_2O$ [+ solvent]	$C_{39.5}H_{37}ClN_2O$
M_r	490.58	591.16
Crystal system, space group	Monoclinic, *C*2/*c*	Monoclinic, $P2_1/c$
Temperature (K)	100(2)	100(2)
a, *b*, *c* (Å)	14.077(2), 20.144(3), 10.359(2)	17.670(4), 15.120(3), 23.890(6)
β (°)	94.94(2)	98.85(2)
V (Å^3)	2926.6 (8)	6307(2)
Z	4	8
Radiation type	Cu *K*α	Cu *K*α
μ (mm^{-1})	0.52	1.33
F(000)	1032	2504
Crystal size (mm)	0.59 × 0.08 × 0.04	0.27 × 0.03 × 0.01
Diffractometer	Rigaku XtaLAB Synergy DW system, HyPix-Arc 150 detector	Agilent Technologies Gemini Ultra with Ruby CCD detector
Absorption correction	Multi-scan	Analytical
T_{min}, T_{max}	0.476, 1.000	0.788, 0.981
No. of measured, independent and observed [$I > 2\sigma(I)$] reflections	26068, 2874, 2649	29556, 10610, 6033
R_{int}	0.025	0.098
$(\sin \theta/\lambda)_{max}$ (Å^{-1})	0.620	0.588
$R[F^2 > 2\sigma(F^2)]$, $wR(F^2)$, S	0.049, 0.125, 1.05	0.063, 0.134, 1.01
No. of reflections	2874	10610
No. of parameters	223	796
No. of restraints	21	0
$\Delta\rho_{max}$, $\Delta\rho_{min}$ (e Å^{-3})	0.37, −0.29	0.24, −0.51

[(a)] Given values do not contain the contribution of the disordered solvent.

Computer programs: *CrysAlis PRO* 1.171.39.46 (Rigaku OD, 2018), SHELXT-2014/7 (Sheldrick, 2015), *SHELXL2014*/7 (Sheldrick, 2015), *PLATON* (Spek, 2009).

Synthetic procedures and analytical data

Solvents and reagents

Dichloromethane was distilled over calcium hydride. $CDCl_3$ was prepared directly before use by running through a basic alumina column. Reagents not listed here were used as received.

Compounds **12** and **13** were obtained as described in literature. [11,12]

Synthesis of 10,15-di(p-tolyl)-21-carba-23-oxaporhyrin **14** *and 10,15-di(p-tolyl)-21-carba-23-oxachlorin* **15**

12 (50 mg, 0.223 mmol), mesitylaldehyde (0.39 mL, 2.68 mmol), **13** (76 mg, 0.246 mmol), and solution of 2 % EtOH in CH_2Cl_2 (100 mL) were placed in a two-necked 250-mL flask. Nitrogen was bubbled through the solution for 15 min, then $Et_2O{:}BF_3$ (28 µL, 0.227 mmol) was added, and the mixture was stirred in the dark for 1 h under N_2. Triethylamine (45 µL, 0.323 mmol) and DDQ (0.27 g, 1.2 mmol) were added and the solution was stirred for a further 1 h. The solvent was evaporated, and the reaction mixture was chromatographed on basic alumina (Brockmann III grade) with dichloromethane as eluant. Product **14** was found in the first fraction, while **15** in the third fraction. **14** was further purified through a chromatographic procedure on basic alumina (Brockmann III grade) with dichloromethane as eluant. Yields: **14,** 12 mg (11%) and **15,** 25 mg (23%).

10,15-Di(p-tolyl)-21-carba-23-oxaporhyrin **14**

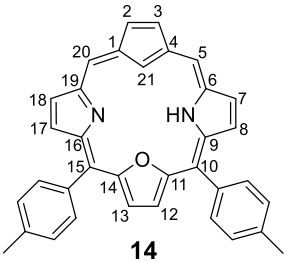

14

UV-vis (CH_2Cl_2): λ_{max} (logε) = 313 (4.4), 410 (4.9), 499 (4.0), 535 (4.0), 608 (3.6), 728 nm (2.7). **^{1}H NMR** (600 MHz, $CDCl_3$, 300 K): δ = 9.79 (s, 2H; H5,20); 8.98 (d, ^3J(H,H) = 4.3 Hz, 2H; H7,18); 8.97 (s, 2H; H12,13); 8.60 (d, ^3J(H,H) = 4.3 Hz , 2H; H8,17); 8.04 (d, ^4J(H,H) = 1.1 Hz, 2H; H2,3); 8.00 (d, ^3J(H,H) = 7.8 Hz, 4H; *o*-Tol); 7.54 (d, ^3J(H,H) = 7,8 Hz, 4H; *m*-Tol); 2.68 (s, 6H; *p*-CH_3(Tol)); –0.41 (s, 1H, NH); –4.30 ppm (s, 1H; H21). **HR-MS** (ESI): *m*/*z* calcd for $C_{35}H_{27}N_2O^+[M+H]^+$: 491,2118; found: 491,2115.

Protonation of 14

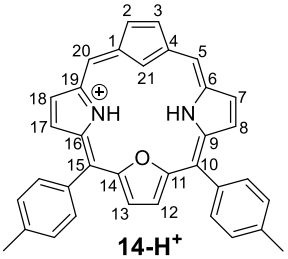

14-H$^+$

14-H$^+$ was obtained by titration of **14** with diluted solution of TFA in chloroform or dichloromethane. **UV-vis** (CH_2Cl_2): λ_{max} (logε) = 296 (4.4), 319 (4.4), 404 (5.0), 467 (4.5), 499 (4.2), 576 (3.9), 612 (4.0), 699 nm (3.6). **^{1}H NMR** (600 MHz, $CDCl_3$, 270 K): δ = 9.97 (s, 2H; H5,20); 9.09 (s, 2H; H12,13); 8.98 (d, ^3J(H,H) = 4.4 Hz, 2H; H7,18); 8.31 (d, ^3J(H,H) = 4.4 Hz, 2H; H8,17); 8.09 (d, ^3J(H,H) = 7.5 Hz, 4H; *o*-Tol); 7.80 (d, ^4J(H,H) = 1.1 Hz, 2H; H2,3); 7.60 (d, ^3J(H,H) = 7.7 Hz, 4H; *m*-Tol); 2.69 (s, 6H; *p*-CH_3(Tol)); 0.43 (s, 1H; NH); –5.84 ppm (s, 1H; H21). **^{13}C NMR** (150.9 MHz, $CDCl_3$, 300 K): δ = 155.8, 142.1, 141.9, 141.7, 139.1, 137.4, 135.1, 130.8, 129.9, 128.6, 127.6, 125.5, 121.1, 118.6, 113.4, 21.5 ppm.

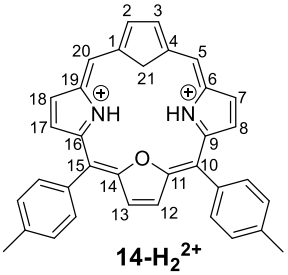

14-H_2^{2+}

14-H_2^{2+} was obtained by addition of concentrated TFA to **14** in chloroform or dichloromethane. **UV-vis** (CH_2Cl_2): λ_{max} (logε) = 341 (4.3), 442 (5.2), 538 (4.1), 607 (3.8), 670 nm (4.1). **^{1}H NMR** (600 MHz, $CDCl_3$, 270 K): δ = 11.25 (s, 2H; H5,20); 10.96 (s, 2H; H2,3); 9.73 (s, 2H; H12,13); 9.58 (d, ^3J(H,H) = 4.6 Hz, 2H; H7,18); 9.07 (d, ^3J(H,H) = 4.6 Hz, 2H; H8,17); 8.31 (d, ^3J(H,H) = 7.7 Hz, 4H; *o*-Tol); 7.82 (d, ^3J(H,H) = 7.7 Hz, 4H; *m*-Tol); 2.79 (s, 6H; *p*-CH_3(Tol)); –1.86 (s, 1H; NH); –7.43 ppm (s, 1H; H21). **^{13}C NMR** (data from HSQC, $CDCl_3$, 280 K): δ = 151.6 (C2,3), 137.4 (*o*-Tol), 134.9 (C8,17), 134.4 (C12,13), 131.7 (C7,18), 129.6 (*m*-Tol), 117.3 (C5,20), 28.4 (C21), 21.6 ppm (*p*-CH_3(Tol)).

10,15-Di(p-tolyl)-21-carba-23-oxachlorin **15**

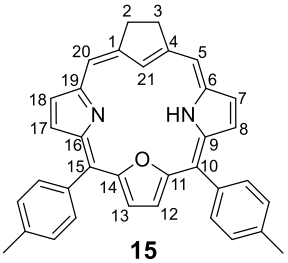

15

UV-vis (CH_2Cl_2): λ_{max} (logε) = 351 (4.3), 402 (5.0), 434 5.0), 518 (4.2), 618 (3.7), 679 nm (4.0). **^{1}H NMR** (600 MHz, $CDCl_3$, 300 K): δ = 9.44 (s, 2H; H5,20); 9.00 (s, 2H; H12,13); 8.93 (d, **^{3}***J*(H,H) = 4.5 Hz, 2H; H7,18); 8.66 (d, **^{3}***J*(H,H) = 4.5 Hz, 2H; H8,17); 8.04 (d, **^{3}***J*(H,H) = 7.7 Hz, 4H; *o*-Tol); 7.54 (d, **^{3}***J*(H,H) = 7.7 Hz, 4H; *m*-Tol); 4.81 (s, 4H; H2,3); 2.70 (s, 6H; *p*-Tol(CH_3)); –1.57 (s, 1H; NH); –4.94 ppm (s, 1H; H21). **HR-MS** (ESI): *m*/*z* calcd for $C_{35}H_{29}N_2O^+$ $[M+H]^+$: 493.2274; found: 493.2310.

Protonation of 15

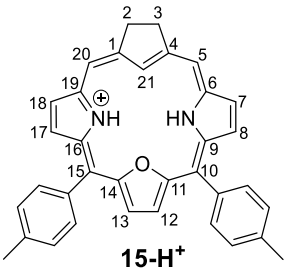

15-H^+

15-H^+ was obtained by titration of **15** with diluted solution of TFA in chloroform or dichloromethane. **UV-vis** (CH_2Cl_2): λ_{max} (logε) = 349 (4.0), 408 (5.2), 439 (5.1), 578 (4.2), 625 nm (4.1). **^{1}H NMR** (600 MHz, $CDCl_3$, 300 K): δ = 9.73 (s, 2H; H5,20); 9.23 (s, 2H; H12,13); 8.96 (d, **^{3}***J*(H,H) = 4.5 Hz, 2H; H7,18); 8.59 (d, **^{3}***J*(H,H) = 4.5 Hz, 2H; H8,17); 8.16 (d, **^{3}***J*(H,H) = 7.7 Hz, 4H; *o*-Tol); 7.62 (d, **^{3}***J*(H,H) = 7.7 Hz, 4H; *m*-Tol); 4.83 (s, 4H; H2,3); 2.71 (s, 6H; *p*-CH_3(Tol)); –1.43 (s, 1H; NH); –6.75 ppm (s, 1H; H21-H). **^{13}C NMR** (150.9 MHz, $CDCl_3$, 300 K): δ = 153.8, 143.6, 138.8, 138.0, 137.5, 135.3, 128.4, 127.1, 126.9, 125.4, 113.1, 109.1, 35.8, 21.6 ppm.

Synthesis of 10,15-dimesityl-21-carba-23-oxaporhyrin **14a and** *10,15-dimesityl-21-carba-23-oxachlorin* **15a**

Macrocycles **14a** and **15a** were synthesized using the same synthetic and purifications procedures as for **14** and **15**, however purification of **14a** required additional chromatography on basic aluminum oxide (Brockmann III grade) with dichloromethane as eluant. Yields: **14a,** 3.6 mg (3%) and **15a,** 19.5 mg (16%).

***10,15-Dimesityl-21-carba-23-oxaporphyrin* 14a**

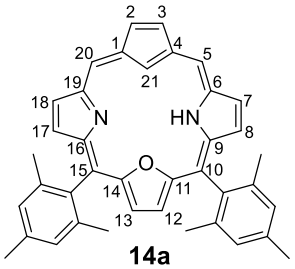

14a

UV-vis (CH_2Cl_2): λ_{max} (logε) = 311 (4.4), 410 (4.8), 536 (4.0), 614 (3.4), 727 nm (3.1). **^{1}H NMR** (600 MHz, CD_2Cl_2, 300 K): δ = 9.76 (s, 2H; H5,20); 8.99 (d, ^3J(H,H) = 4.4 Hz, 2H; H7,18); 8.83 (s, 2H; H12,13); 8.32 (d, ^3J(H,H) = 4.4 Hz, 2H; H8,17); 8.08 (d, ^4J(H,H) = 1.4 Hz, 2H; H2,3); 7.31 (s, 4H; *m*-Mes); 2.61 (s, 6H; *p*-Mes(CH_3)); 1.84 (s, 6H; *o*-Mesl(CH_3)); –4.12 ppm (s, 1H; H21). NH is invisible. **HR-MS** (ESI): *m*/*z* calcd for $C_{39}H_{35}N_2O^+$ $[M+H]^+$: 547.2750; found: 547.2755.

Protonation of 14a

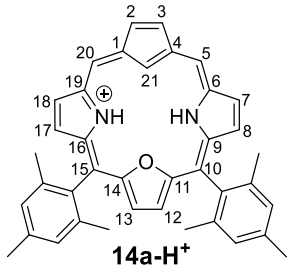

14a-H$^+$

14a-H$^+$ was obtained by titration of **14a** with diluted solution of TFA in chloroform or dichloromethane. **UV-vis** (CH_2Cl_2): λ_{max} (logε) = 322 (4.4), 401 (4.9), 467 (4.5), 501 (4.3), 575 (3.9), 611 nm (3.9). **^{1}H NMR** (600 MHz, CD_2Cl_2, 300 K): δ = 10.03 (s, 2H; H5,20); 9.09 (d, ^3J(H,H) = 4.4 Hz, 2H; H7,18); 8.92 (s, 2H; H12,13); 8.32 (d, ^3J(H,H) = 4.4 Hz, 2H; H8,17); 7.87 (d, ^4J(H,H) = 1.4 Hz, 2H; H2,3); 7.33 (s, 4H; *m*-Mes); 2.61 (s, 6H; *p*-Mes(CH_3)); 1.83 (s, 6H; *o*-Mesl(CH_3)); 0.49 (s, 1H; NH); –5.50 ppm (s, 1H; H21). **^{13}C NMR** (150.9 MHz, CD_2Cl_2, 300 K): δ = 155.3, 142.7, 142.2, 141.8, 140.4, 139.8, 136.0, 131.1, 129.9, 129.5, 129.1, 125.4, 122.2, 119.3, 111.4, 21.8, 21.0 ppm.

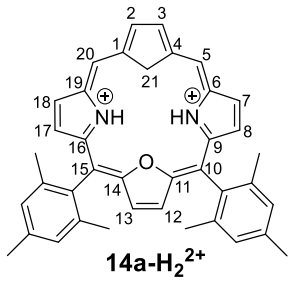

14a-H$_2^{2+}$

14a-H$_2^{2+}$ was obtained by addition of concentrated TFA to **14a** in chloroform or dichloromethane. **UV-vis** (CH_2Cl_2): λ_{max} (logε) = 395 (5.3), 528 (4.0), 568 (3.8), 594 (3.8), 651 nm (3.8). **^{1}H NMR** (600 MHz, $CDCl_3$, 270 K): δ = 11.56 (s, 2H; H5,20); 11.22 (s, 2H; H2,3); 9.83 (s, 2H; H12,13); 9.82 (d, ^3J(H,H) = 4.2 Hz, 2H; H7,18);

9.22 (d, ^3J(H,H) = 4.2 Hz, 2H; H8,17); 7.42 (s, 4H; *m*-Mes); 2.67 (s, 6H; *p*-Mes(CH_3)); 1.73 (s, 6H; *o*-Mes(CH_3)); –3.00 (s, 1H; NH); –7.93 ppm (s, 1H; H21).

10,15-Dimesityl-21-carba-23-oxachlorin **15a**

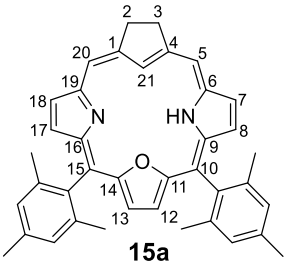

15a

UV-vis (CH_2Cl_2): λ_{max} (logε) = 351 (4.3), 402 (5.0), 435 (5.0), 519 (4.1), 618 (3.6), 681 nm (3.9). **^{1}H NMR** (600 MHz, $CDCl_3$, 300K): δ = 9.35 (s, 2H; H5,20); 8.85 (d, ^3J(H,H) = 4.4 Hz, 2H; H7,18); 8.77 (s, 2H; H12,13); 8.48 (d, ^3J(H,H) = 4.7 Hz, 2H; H8,17); 7.20 (s, 4H; *m*-Mes); 4.75 (s, 2H; H2,3); 2.58 (s, 6H; *p*-CH_3(Mes)); 1.78 (s, 12H; *o*-CH_3(Mes)); −1.41 (br s, 1H; NH); −4.81 ppm (s, 1H, H21). **HR-MS** (ESI): *m*/*z* calcd for $C_{39}H_{37}N_2O^+$ $[M+H]^+$: 549.2906, found: 549.2910.

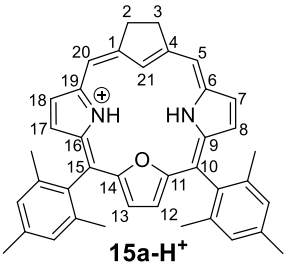

15a-H$^+$

15a-H$^+$ was obtained by titration of **15a** with diluted solution of TFA in chloroform or dichloromethane. **UV-vis** (CH_2Cl_2): λ_{max} (logε) = 348 (4.0), 408 (5.2), 442 (5.1), 580 (4.1), 627 nm (4.0). **^{1}H NMR** (600 MHz, $CDCl_3$, 300K): δ = 9.68 (s, 2H; H5,20); 8.98 (s, 2H; H12,13); 8.91 (d, ^3J(H,H) = 4.5 Hz, 2H; H7,18); 8.48 (d, ^3J(H,H) = 4.5 Hz, 2H; H8,17); 7.17 (s, 4H, *m*-Mes); 4.77 (s, 2H; H2,3); 2.56 (s, 6H; *p*-CH_3(Mes)); 1.72 (s, 12H; *o*-CH_3(Mes)); −1.23 (s, 1H; NH); −6.62 (s, 1H; H21) ppm.**^{13}C NMR** (150.9 MHz, $CDCl_3$, 300K): δ = 153.8, 152.3, 143.6, 140.0, 138.8, 138.7, 136.7, 136.3, 128.4, 126.2, 126.1, 125.9, 110.2, 109.3, 35.8, 21.5, 20.7 ppm.

10,15-Dimesityl-21-carbachlorin **16**

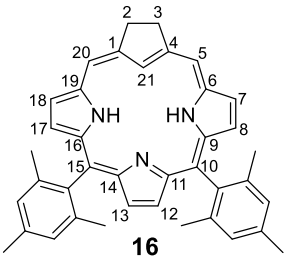

16

Pyrrole (93 µL, 1.34 mmol), mesitylaldehyde (0.39 mL, 2.68 mmol), **12** (0.15 g, 0.67 mmol), and solution of 3 % EtOH in $CHCl_3$ (300 mL) were placed in a 500-mL flask. Nitrogen was bubbled through the solution for 30 min, then $Et_2O{:}BF_3$ (83 µL,0.67 mmol) was added, and the mixture was stirred in the dark for 1 h under N_2. Triethylamine (0.11 mL, 0.74 mmol) and *p*-chloranil (0.98 g, 4.0 mmol) were added and the solution was stirred for a further 1 h. The solvent was evaporated, and the reaction mixture was purified by recrystalization from CH_2Cl_2/hexane. The filtrate (product **16**) was further purified through a chromatographic procedure on silica gel with MeOH/CH_2Cl_2 (2:98 V/V) as eluant. The third fraction was identified as compound **16**, which was finally purified by chromatography on basic aluminum oxide with CH_2Cl_2 as eluant (3.8 mg, 1.04 %). **UV-vis** (CH_2Cl_2): λ_{max} (logε) = 372 (4.4), 402 (4.9), 419 (5.2), 510 (4.1), 536 (3.7), 596 (3.7), 652 nm (3.9). **^{1}H**

NMR (600 MHz, CD_2Cl_2, 300 K): δ = 9.21 (s, 2H; H5,20); 8.91 (d, ^3J(H,H) = 4.6 Hz, 2H; H7,18); 8.54 (d, ^3J(H,H) = 4.6 Hz, 2H, H8,17); 8.39 (s, 2H; H12,13); 7.26 (s, 4H; 10,15-*m*-Mes); 4.76 (s, 4H; H2,3); 2.60 (s, 6H; 10,15-*p*-CH_3(Mes)); 1.83 (s, 12H; 10,15-*o*-CH_3(Mes)); –3.06 (br s, 1H; NH); –6.42 ppm (s, 1H; H21). **^{13}C NMR** (150.9 MHz, $CDCl_3$, 300 K): δ = 151.8, 149.2, 139.3, 138.5, 137.9, 137.3, 134.2, 131.3, 127.7, 124.6, 123.8, 123.1, 116.8, 100.9, 35.3, 21.42, 21.36 ppm. **HR-MS** (ESI): *m*/*z* calcd for $C_{39}H_{38}N_3^+$ $[M+H]^+$: 548.3060; found: 548.3013.

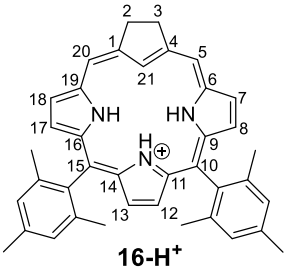

16-H$^+$

16-H$^+$ was obtained by titration of **16** with diluted solution of TFA in dichloromethane. **UV-vis** (CH_2Cl_2): λ_{max} (logε) = 420 (5.1), 438 (5.0), 559 (4.0), 587 (4.2), 636 nm (3.8).**^{1}H NMR** (600 MHz, CD_2Cl_2, 300 K): δ = 9.61 (s, 2H; H5,20); 9.02 (d, ^3J(H,H) = 4.6 Hz, 2H; H7,18); 8.69 (d, ^3J(H,H) = 4.6 Hz, 2H, H8,17); 8.67 (s, 2H; H12,13); 7.33 (s, 4H; 10,15-*m*-Mes); 4.85 (s, 4H; H2,3); 2.62 (s, 6H; 10,15-*p*-CH_3(Mes)); 1.79 (s, 12H; 10,15-*o*-CH_3(Mes)); –2.65 (s, 2H; NH); –4.89 (s, 1H; NH); –6.50 ppm (s, 1H; H21).

10,15-Di(p-tolyl)-21-oxo-21-carba-23-oxaporphyrinoids 17 and 18

10,15-Di(p-tolyl)-21-oxo-21-carba-23-oxaporphyrin 17

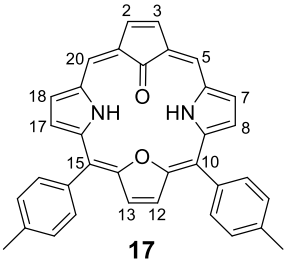

17

Macrocycle **17** was achieved as a side product in the synthesis of 10,15-ditolyl-21-carba-23-oxaporphyrinoids with the use of DDQ as oxidant. Initially, **17** was eluted with **14** in the first fraction during chromatographic procedure on basic aluminum oxide (Brockmann III grade; CH_2Cl_2). Final separation by chromatography on basic aluminum oxide (Brockmann III grade) with $CHCl_3$ as eluant gave **9** in trace amount (<1%). **UV-vis** (CH_2Cl_2): λ_{max} = 369, 624, 671 nm. **^{1}H NMR** (600 MHz, $CDCl_3$, 300K): δ = 13.34 (s, 2H; NH); 7.28 (d, ^3J(H,H) = 7.9 Hz, 4H; *o*-Tol); 7.20 (d, ^3J(H,H) = 7.9 Hz, 4H, *m*-Tol); 6.61 (dd, ^3J(H,H) = 4.1 Hz, ^4J(H,H) = 1.8 Hz, 2H; H7,18); 6.42 (s, 2H; H12,13); 6.38 (s, 2H; H5,20); 5.93 (dd, ^3J(H,H) = 4.1 Hz, ^4J(H,H) = 2.3 Hz, 2H; H8,17); 5.31 (s, 2H; H2,3); 2.40 ppm (s, 6H; *p*-CH_3(Tol)). **^{13}C NMR** (data from HSQC and HMBC, $CDCl_3$, 300 K): δ = 195.5 (C21), 132.2 (*o*-Tol), 129.5 (C2,3), 129.2 (*m*-Tol), 128.4 (C12,13), 122.0 (C7,18), 121.4 (C5,20), 118.8 (C8,17), 21.3 ppm (*p*-CH_3(Tol)). **HR-MS** (ESI): *m*/*z* calcd for $C_{35}H_{26}N_2O_2^+$ $[M]^+$: 506.1989; found: 506.1958.

In solution the compound **17** was unstable and its decomposition during long ^{13}C and 2D NMR measurements was observed.

10,15-Di(p-tolyl)-21-oxo-21-carba-23-oxachlorin 18

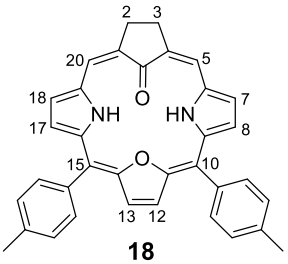

18

10,15-Di(p-tolyl)-21-carba-23-oxachlorin **15** (6.7 mg, 0.014 mmol) was dissolved in 10 ml of dichloromethane and AgOAc (8.5 mg, 0.05 mmol) dissolved in 7 ml of methanol was added. The mixture was stirred at reflux for 1 h. The reaction progress was monitored by UV-Vis spectroscopy. The solvent was evaporated, and the reaction mixture was purified by chromatography on silica gel column with CH_2Cl_2 as eluant. The first fraction was identified as compound **18** (1.8 mg, 25%). **UV-vis** (CH_2Cl_2): λ_{max} (logε) = 311 (4.3), 378 (4.3), 430 (5.1), 448 (5.1), 542 (3.7) , 561 (3.7), 603 (3.7), 613 (3.8), 657 nm (4.2). **^{1}H NMR** (600 MHz, CD_2Cl_2, 300K): δ = 9.29 (s, 2H; H5,20); 8.65 (s, 2H; H12,13); 8.50 (dd, ^3J(H,H) = 4.4 Hz, ^4J(H,H) = 1.4 Hz, 2H; H7,18); 8.03 (dd, ^3J(H,H) = 4.4 Hz, ^4J(H,H) = 2.2 Hz, 2H; H8,17); 7.99 (d, ^3J = 8.0 Hz, 4H; o-Tol); 7.56 (d, ^3J = 8.0 Hz, 4H, *m*-Tol); 4.53 (s, 4H; H2,3); 2.91 (s, 2H; NH); 2.67 ppm (s, 6H, *p*-CH_3(Tol)). **^{13}C NMR** (150.9 MHz, $CDCl_3$, 300K): δ = 179.1, 152.1, 138.6, 137.7, 135.9, 133.9, 133.4, 130.3, 128.3, 125.6, 122.2, 121.9, 118.2, 108.2, 30.6, 21.5 ppm. **HR-MS** (ESI): *m*/*z* calcd for $C_{35}H_{28}N_2O_2^+$ $[M]^+$: 508.2151; found: 508.2153.

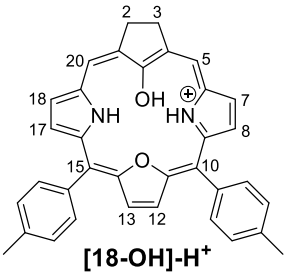

[18-OH]-H$^+$

[18-OH]-H$^+$ was obtained by titration of **18** with diluted solution of TFA in dichloromethane. **UV-vis** (CH_2Cl_2): λ_{max} (logε) = 291 (4.3), 409 (5.1), 440 (5.0), 581 (4.0), 627 nm (3.8). **^{1}H NMR** (600 MHz, CD_2Cl_2, 220K): δ = 9.82 (s, 2H; H5,20); 9.48 (s, 2H; H12,13); 9.35 (d, ^3J(H,H) = 3.8 Hz, 2H; H7,18); 8.98 (d, ^3J(H,H) = 3.8 Hz, 2H; H8,17); 8.11 (d, ^3J = 7.6 Hz, 2H; o-Tol); 8.05 (d, ^3J = 7.2 Hz, 2H; o-Tol); 7.66 (d, ^3J = 7.6 Hz, 2H, *m*-Tol); 7.64 (d, ^3J = 7.2 Hz, 2H, *m*-Tol); 5.14 (d, ^2J = 13.7 Hz, 2H; H2,3); 4.22 (d, ^2J = 13.7 Hz, 2H; H2',3'); 2.70 (s, 6H, *p*-CH_3(Tol)); –4.59 ppm (s, 2H; NH).

Results and Discussion

Schemes

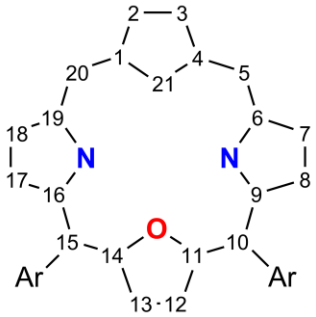

Scheme S1 Atoms numerations (all hydrogen atoms are omitted).

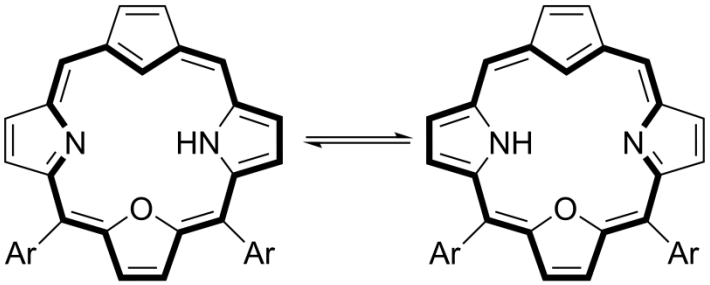

Scheme S2 Tautomers of 10,15-diaryl-21-carba-23-oxaporphyrin **14**.

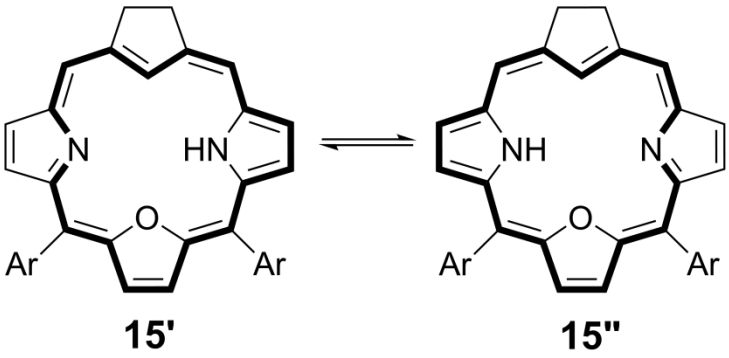

Scheme S3 Tautomers of 10,15-diaryl-21-carba-23-oxachlorin **15**.

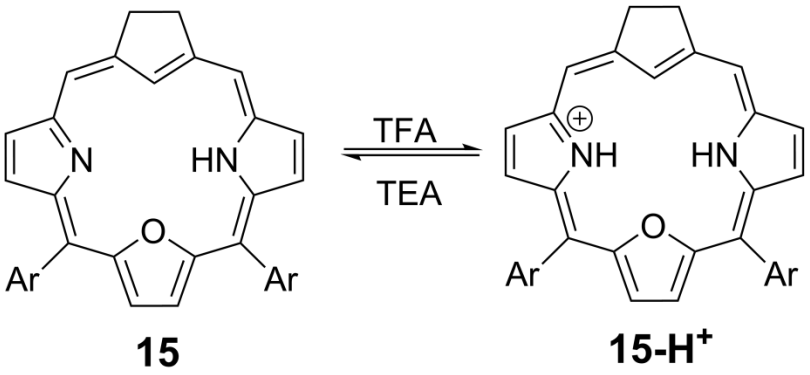

Scheme S4 Protonation of 10,15-diaryl-21-carba-23-oxachlorin **15**.

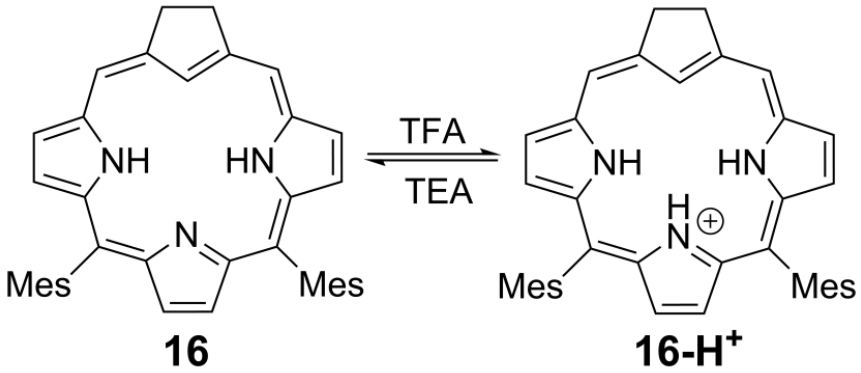

Scheme S5 Protonation of 10,15-dimesityl-21-carbachlorin **16**.

X-ray structures

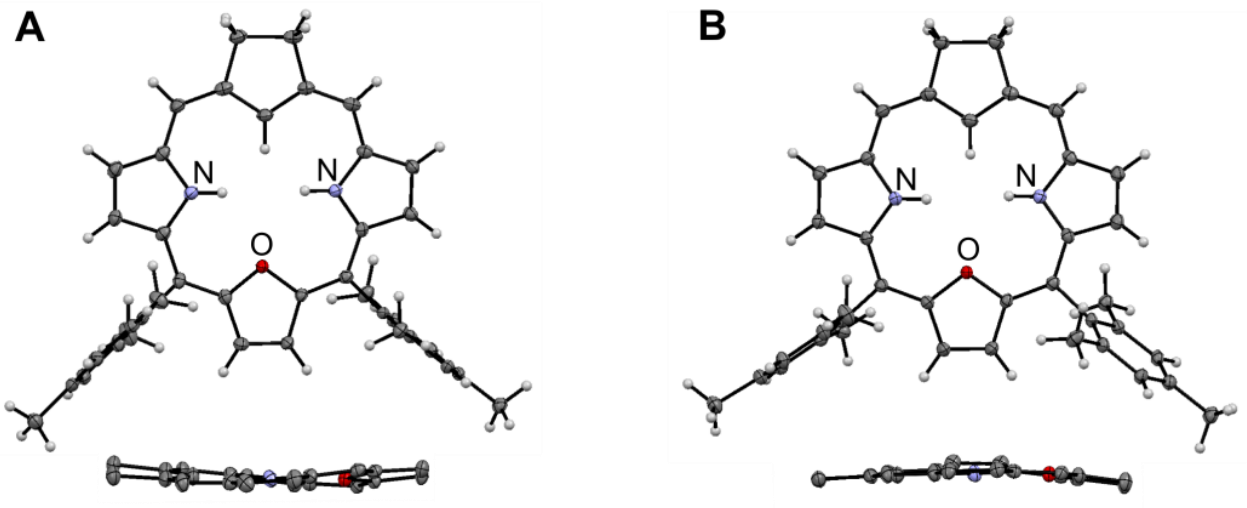

Fig. S1 Molecular structures of **15a**. Two crystallographically different molecules are present in the crystal: ruffled (A) and saddle (B) Top: perspective view; bottom: side view (*meso*-mesityl groups and H atoms are omitted for clarity). Displacement ellipsoids represent the 30% probability. Site occupation factors of N-bound H atoms are 0.5.

^{1}H NMR spectra

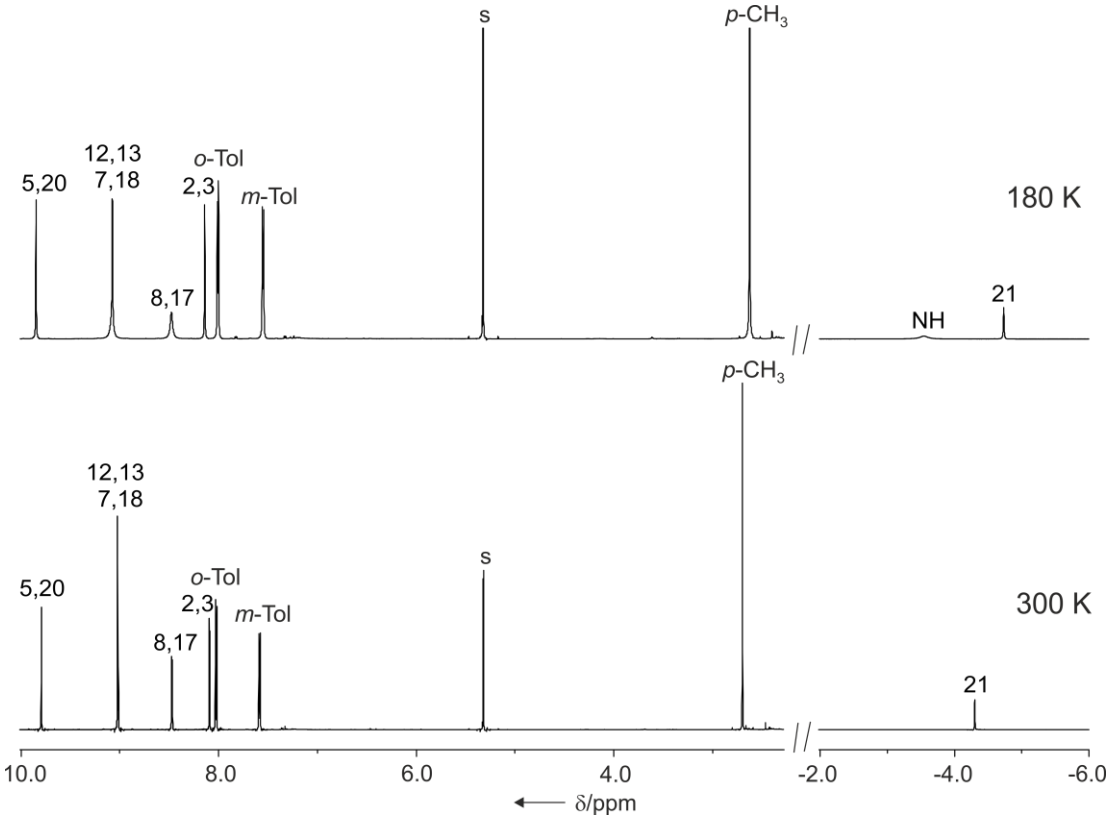

Fig. S2 ^{1}H NMR spectra of **14** at 300 K (bottom) and 180 K (top) (600 MHz, CD_2Cl_2).

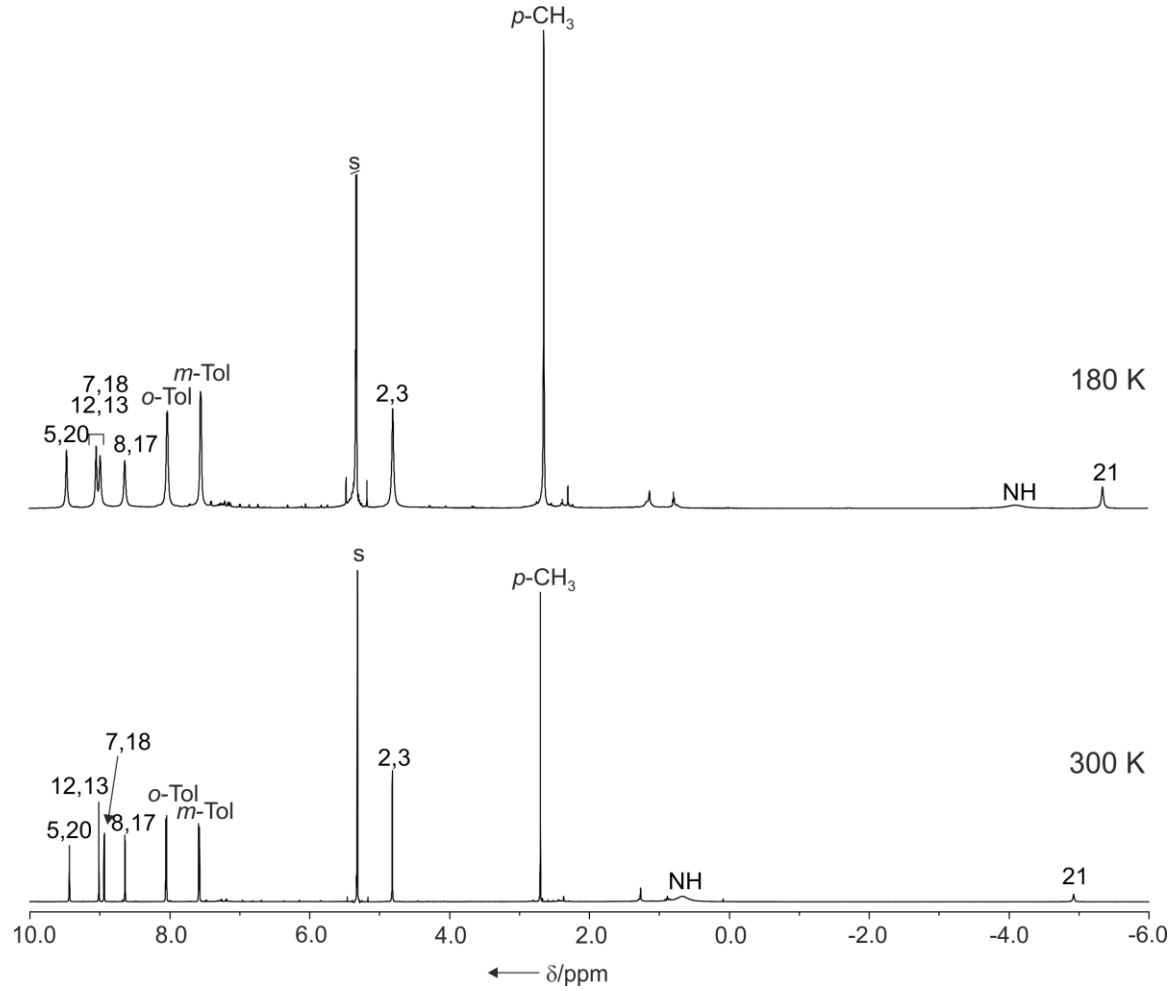

Fig. S3 ^{1}H NMR spectra of **15** at 300 K (bottom) and 180 K (top) (600 MHz, CD_2Cl_2).

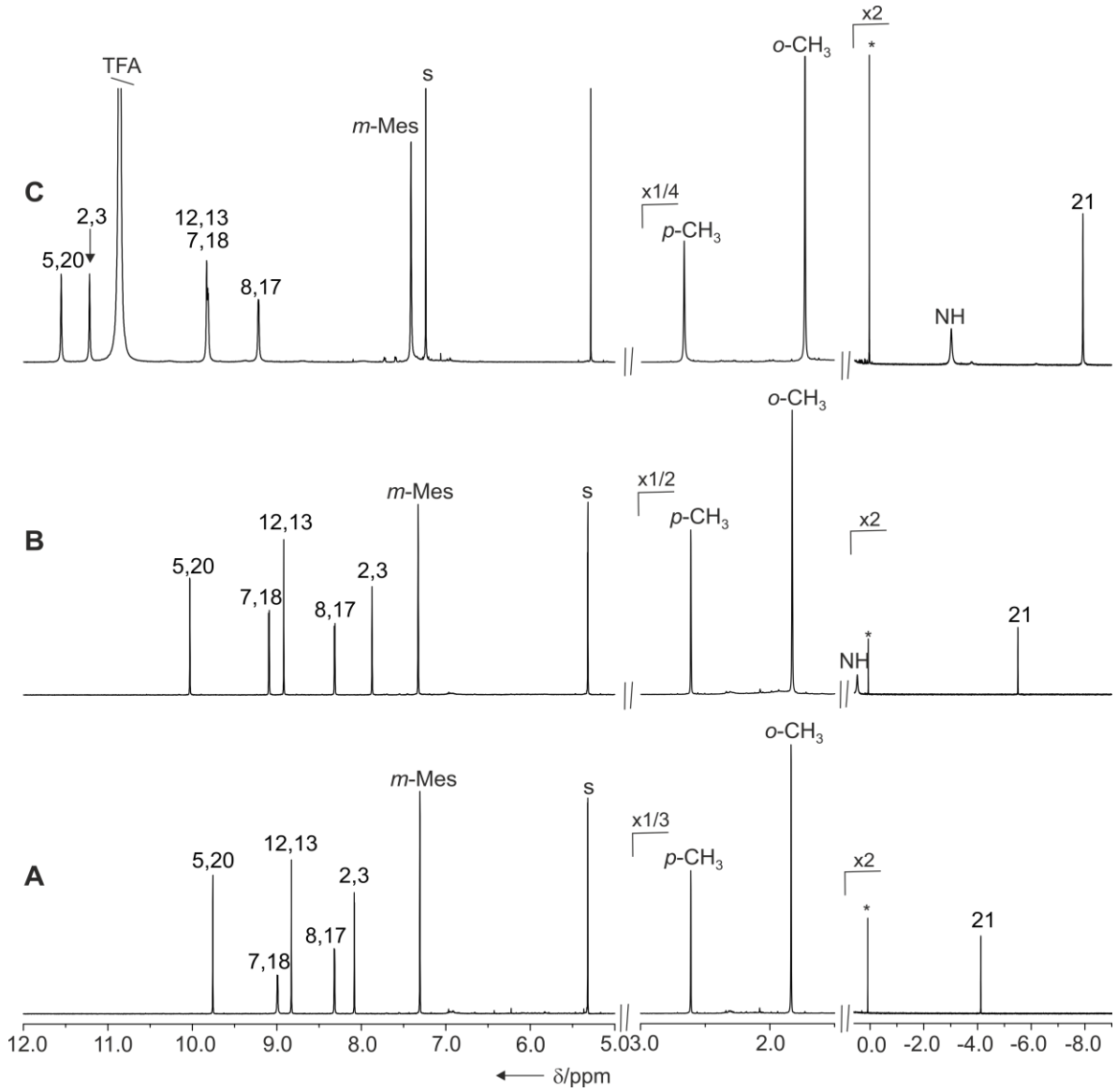

Fig. S4 ^{1}H NMR spectra of A) **14a** (600 MHz, CD_2Cl_2, 300 K), B) **14a-H$^+$** (600 MHz, CD_2Cl_2, 300 K) and C) **14a-H$_2^{2+}$** (600 MHz, $CDCl_3$, 270 K).

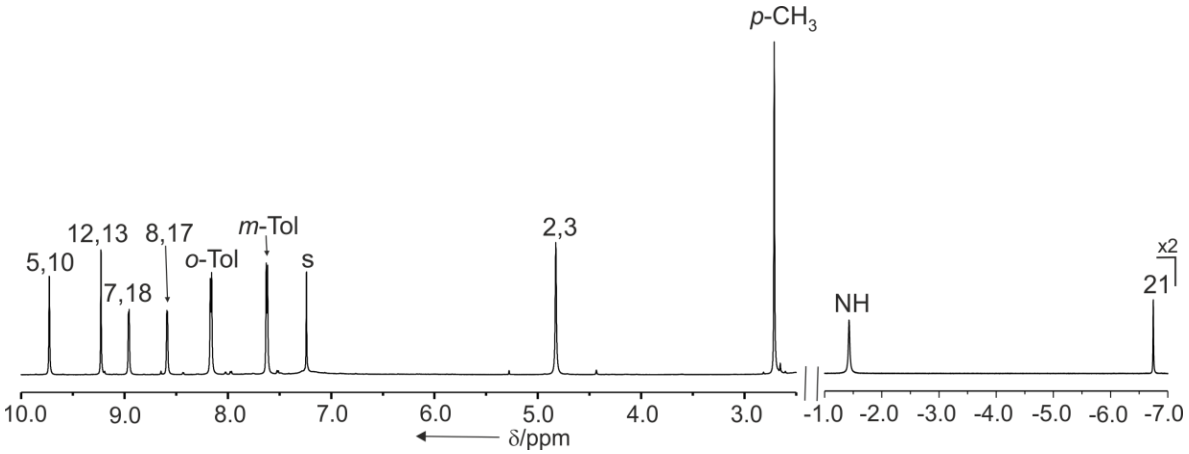

Fig. S5 ^{1}H NMR spectra of **15-H$^+$** (600 MHz, $CDCl_3$, 300 K).

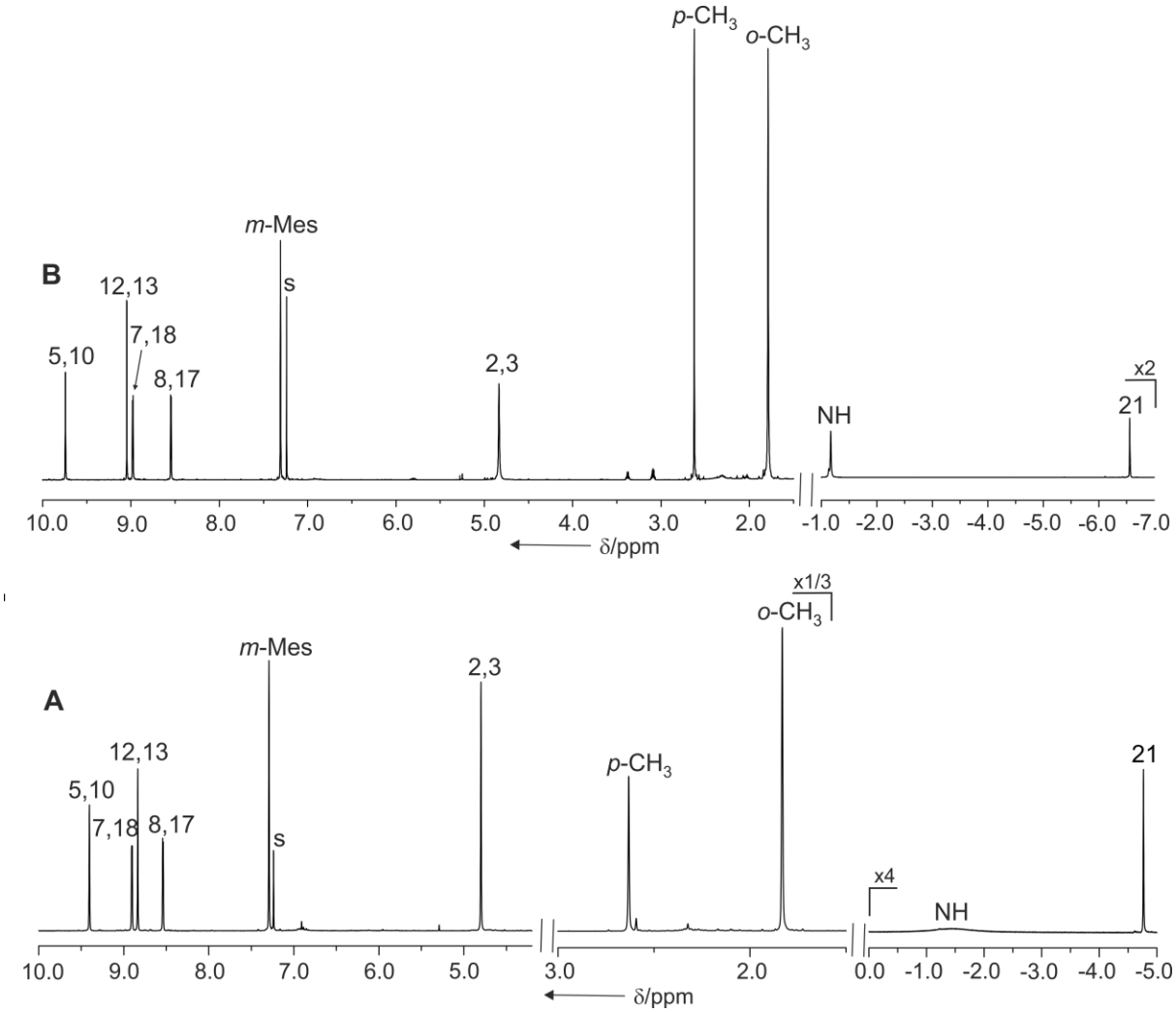

Fig. S6 ^{1}H NMR spectra of A) **15a** and B) **15a-H^{+}** (600 MHz, $CDCl_3$, 300 K).

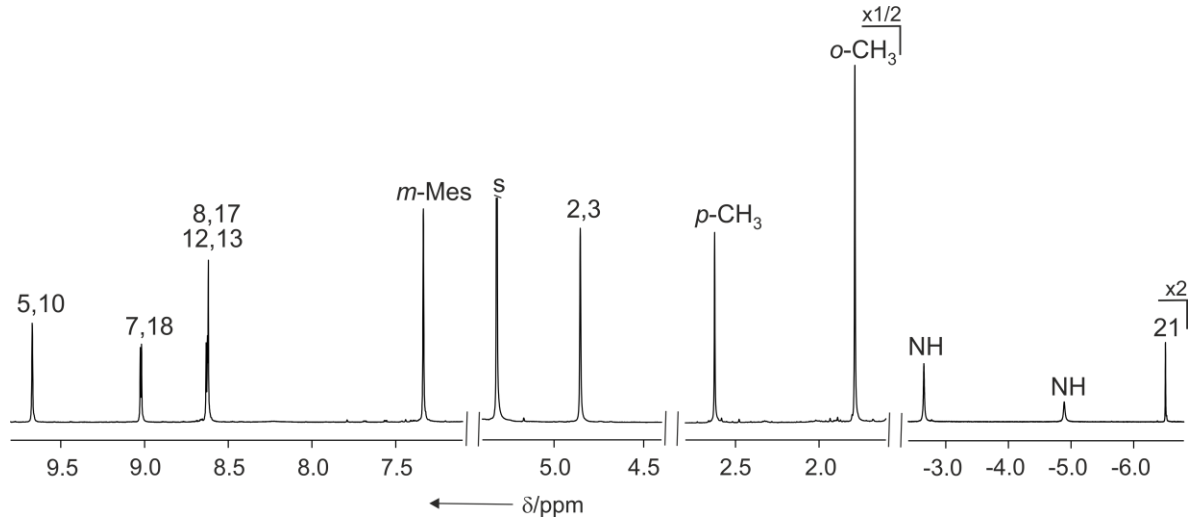

Fig. S7 ^{1}H NMR spectrum of **16-H^{+}** (600 MHz, CD_2Cl_2, 300 K).

^{13}C NMR spectra

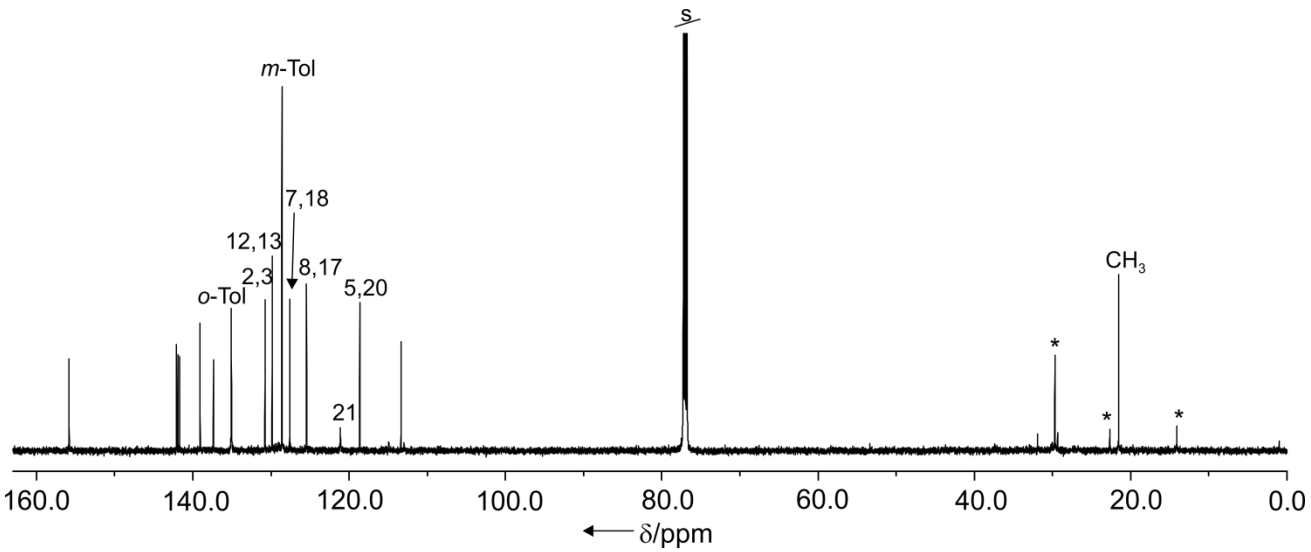

Fig. S8 ^{13}C NMR spectrum of **14-H$^+$** (150.9 MHz, $CDCl_3$, 300 K).

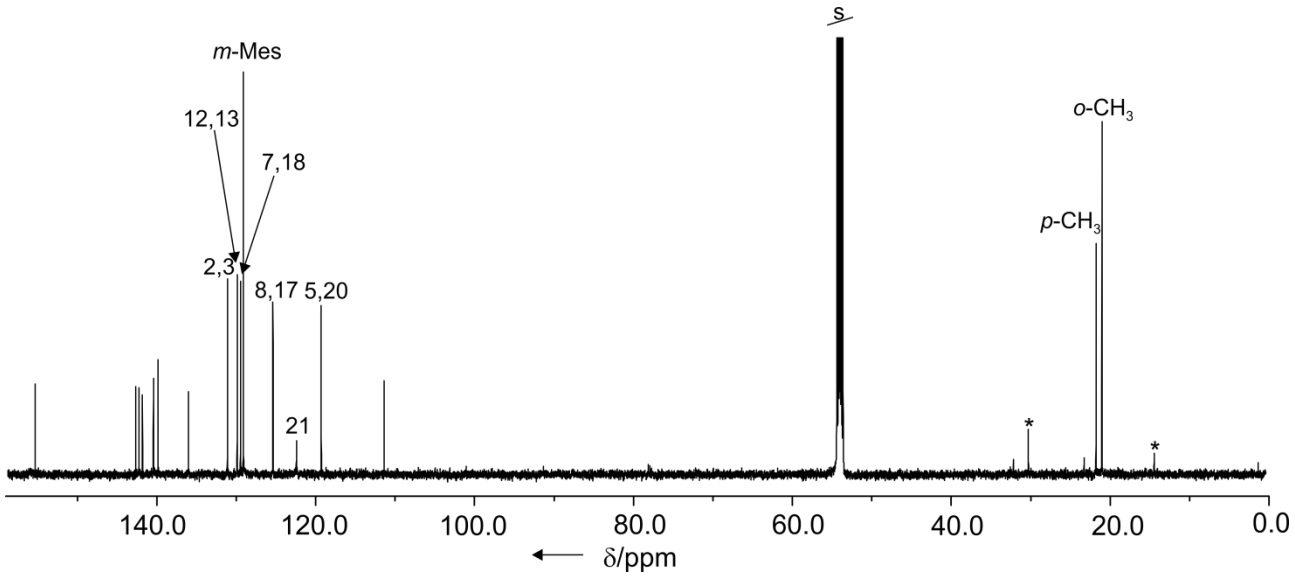

Fig. S9 ^{13}C NMR spectrum of **14a-H$^+$** (150.9 MHz, CD_2Cl_2, 300 K).

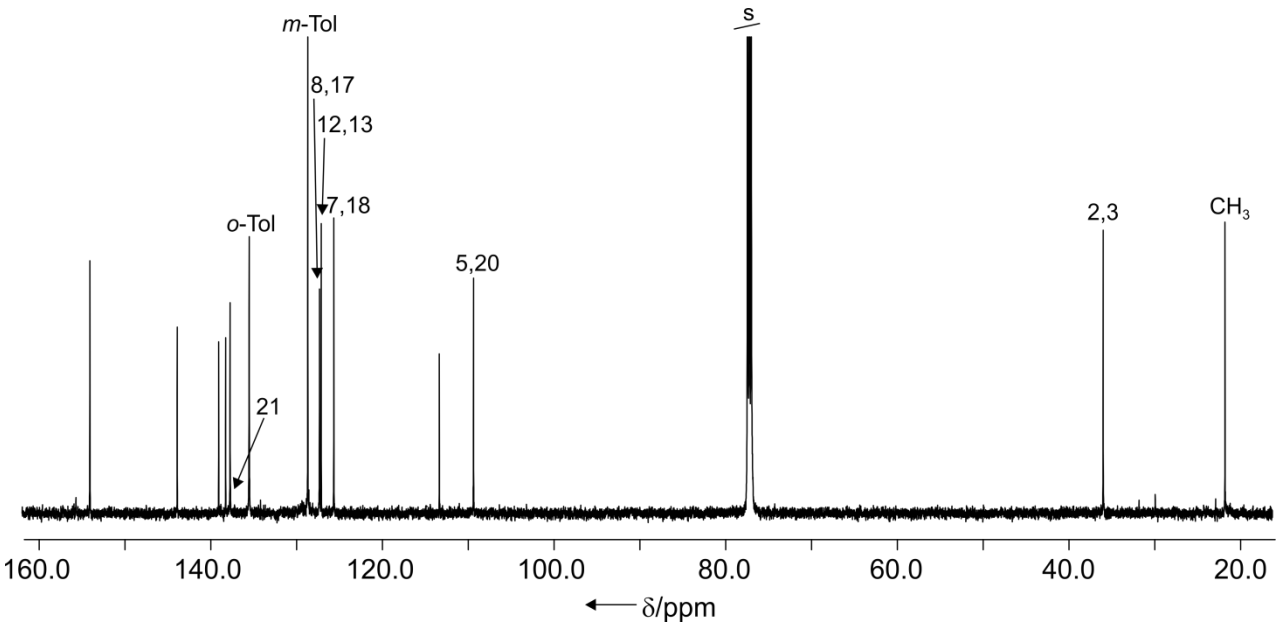

Fig. S10 ^{13}C NMR spectrum of **15-H$^+$** (150.9 MHz, $CDCl_3$, 300 K).

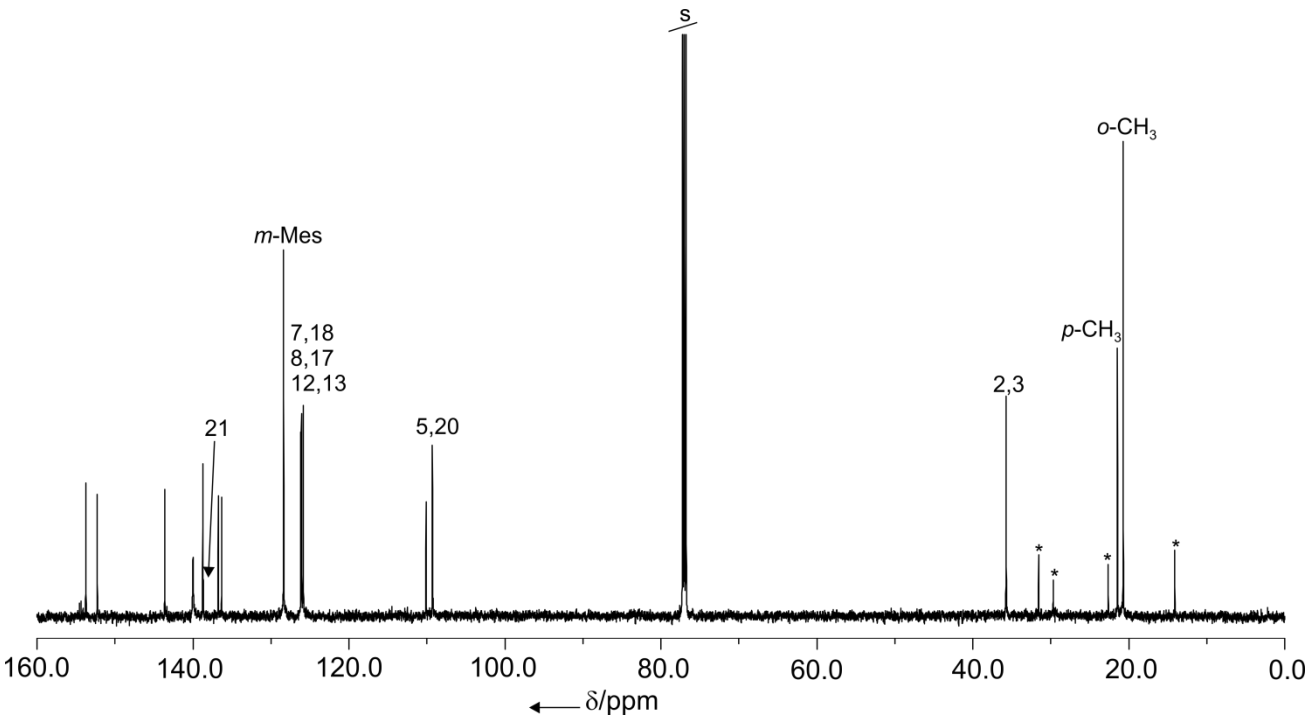

Fig. S11 ^{13}C NMR spectrum of **15a-H$^+$** (150.9 MHz, $CDCl_3$, 300 K).

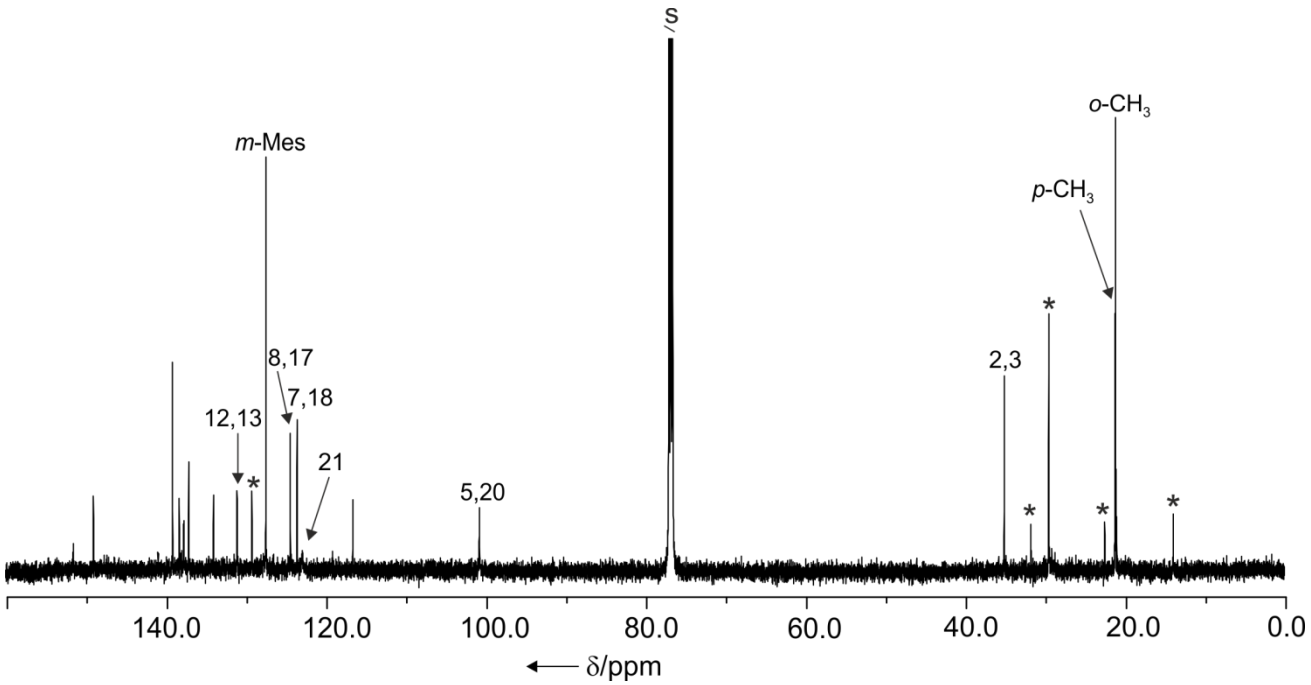

Fig. S12 ^{13}C NMR spectrum of **16** (150.9 MHz, $CDCl_3$, 300 K).

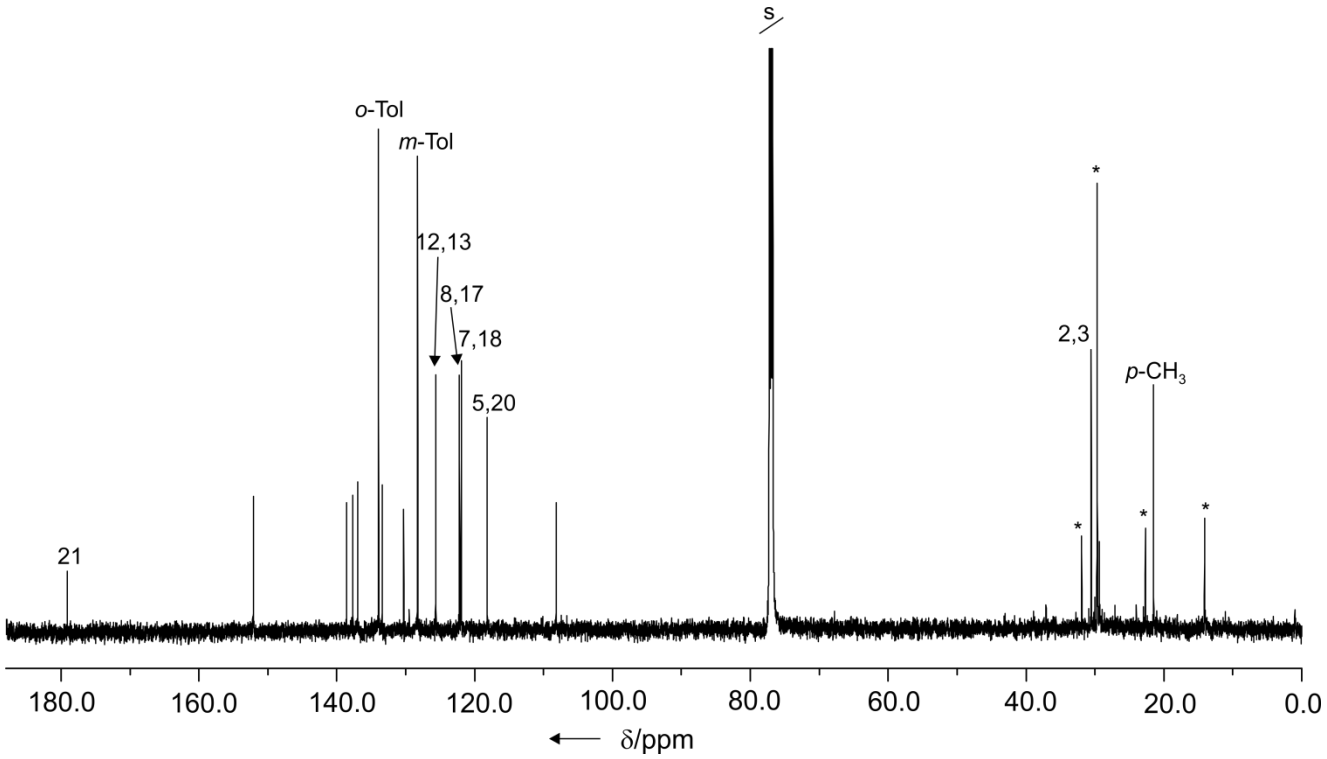

Fig. S13 ^{13}C NMR spectrum of **18** (150.9 MHz, $CDCl_3$, 300 K).

2D NMR spectra

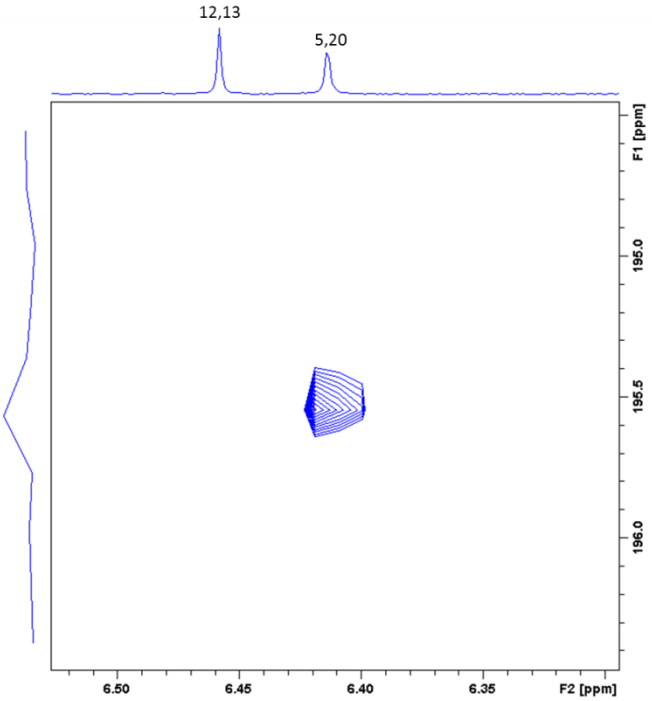

Fig. S14 Crucial fragment of HMBC spectrum of **17** (600 MHz, CD_2Cl_2, 300 K).

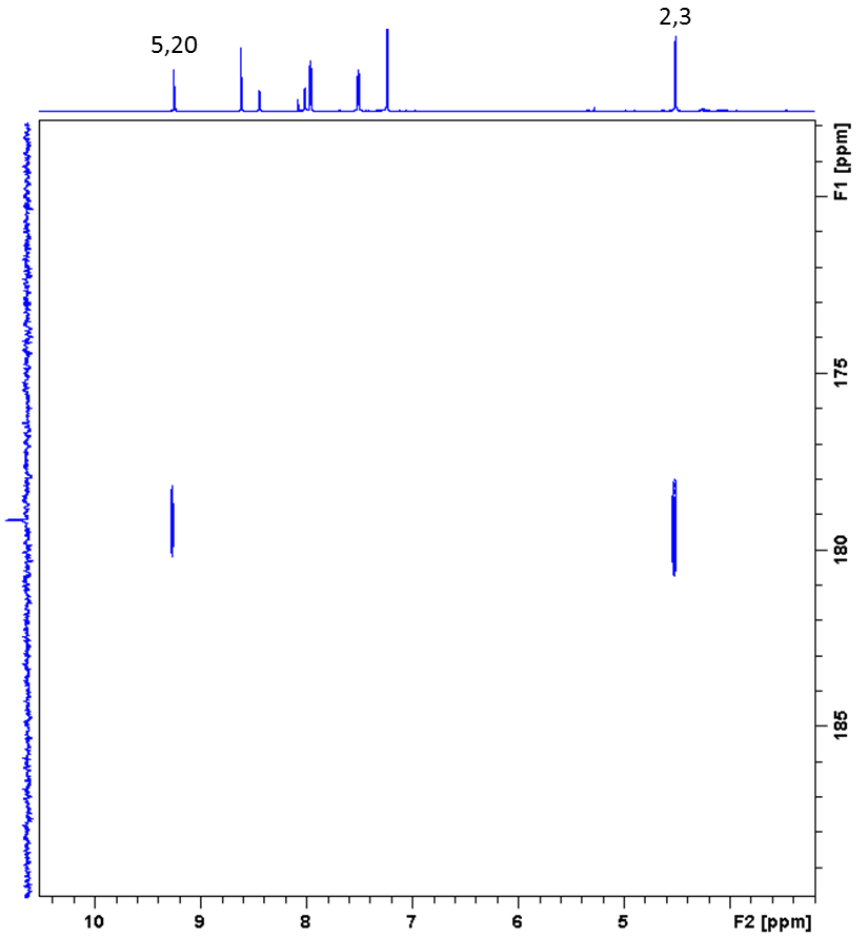

Fig. S15 Crucial fragment of HMBC spectrum of **18** (600 MHz, $CDCl_3$, 300 K).

UV-vis spectra

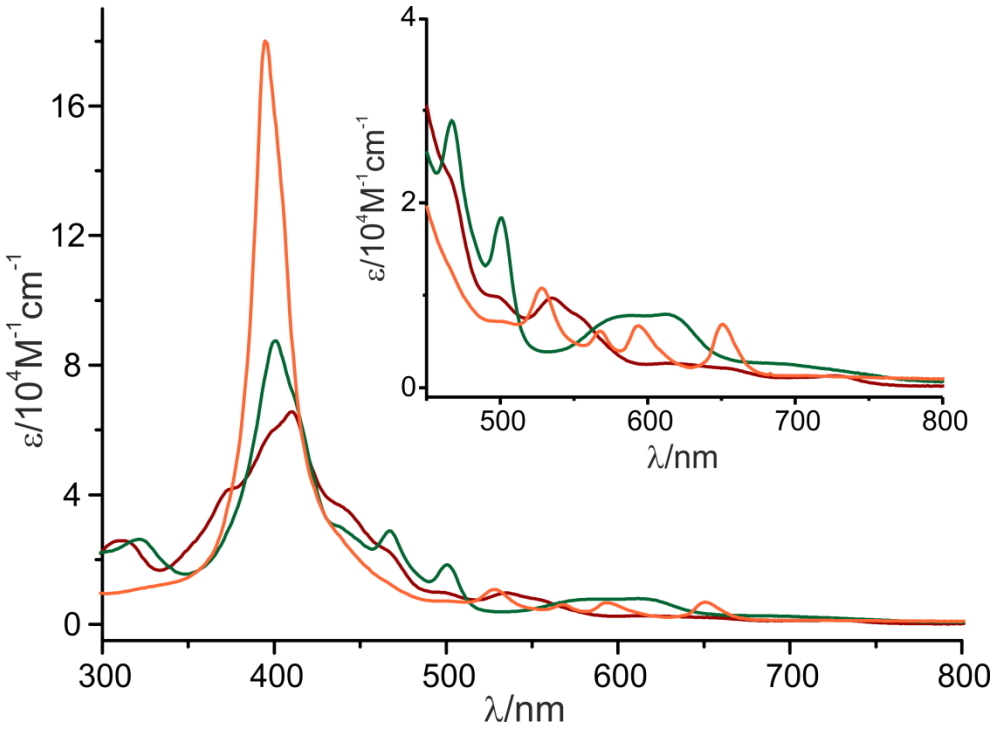

Fig. S16 The electronic absorption spectra (CH_2Cl_2) of **14a** (red line), **14a-H$^+$** (green line) and **14a-H$_2^{2+}$** (orange line).

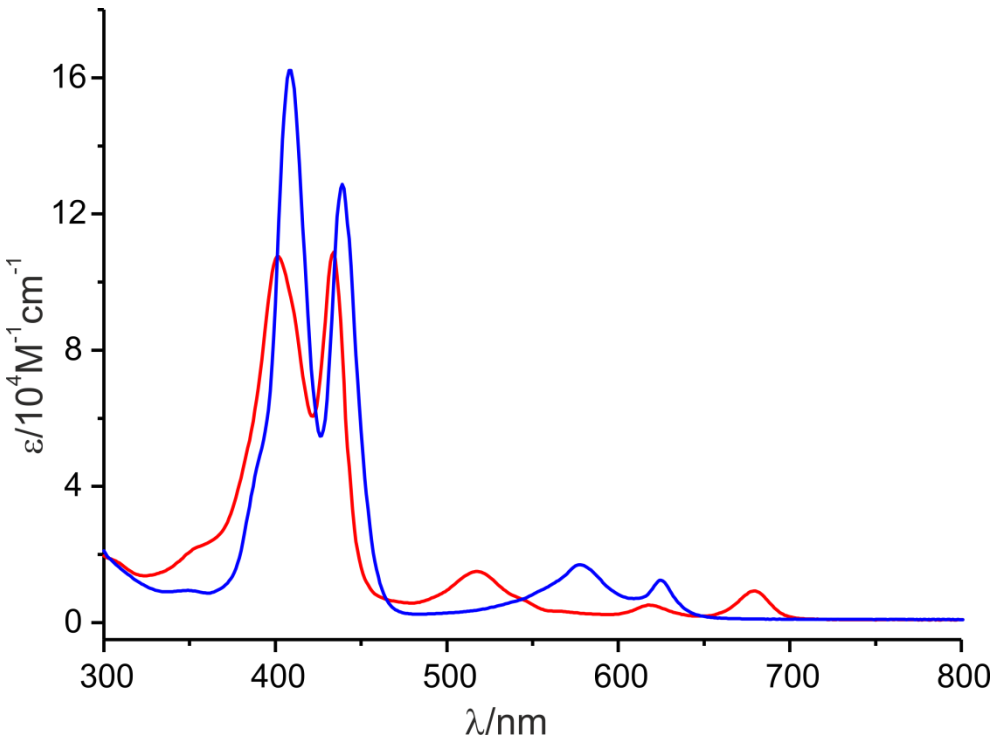

Fig. S17 The electronic absorption spectra (CH_2Cl_2) of **15** (red line) and **15-H$^+$** (blue line).

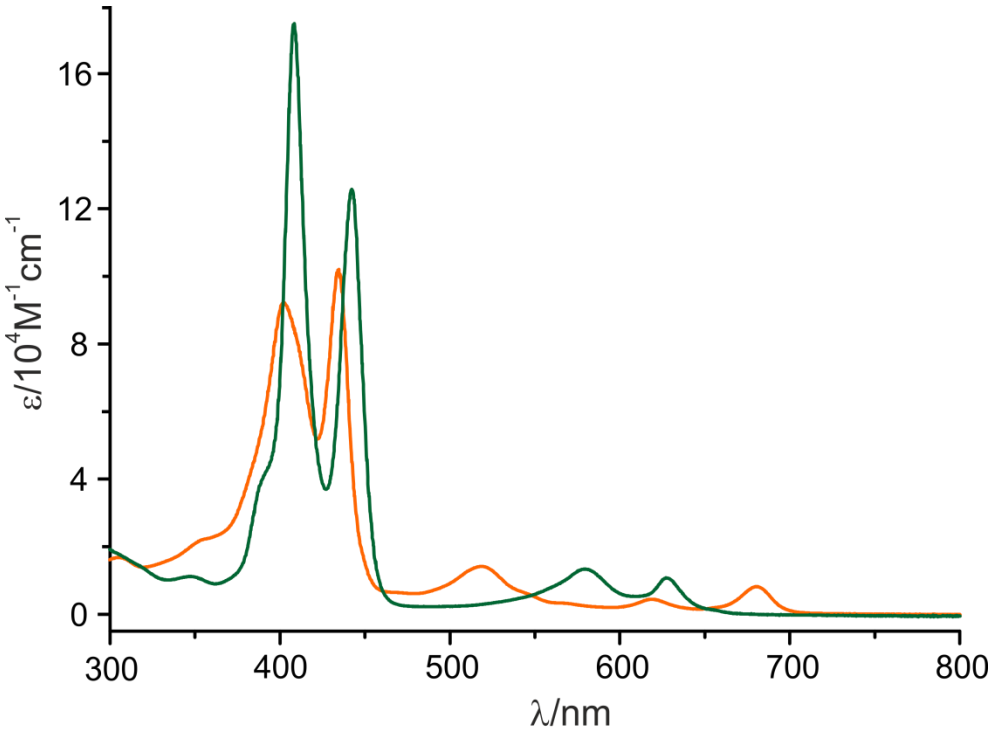

Fig. S18 The electronic absorption spectra (CH_2Cl_2) of **15a** (orange line) and **15a-H⁺** (green line).

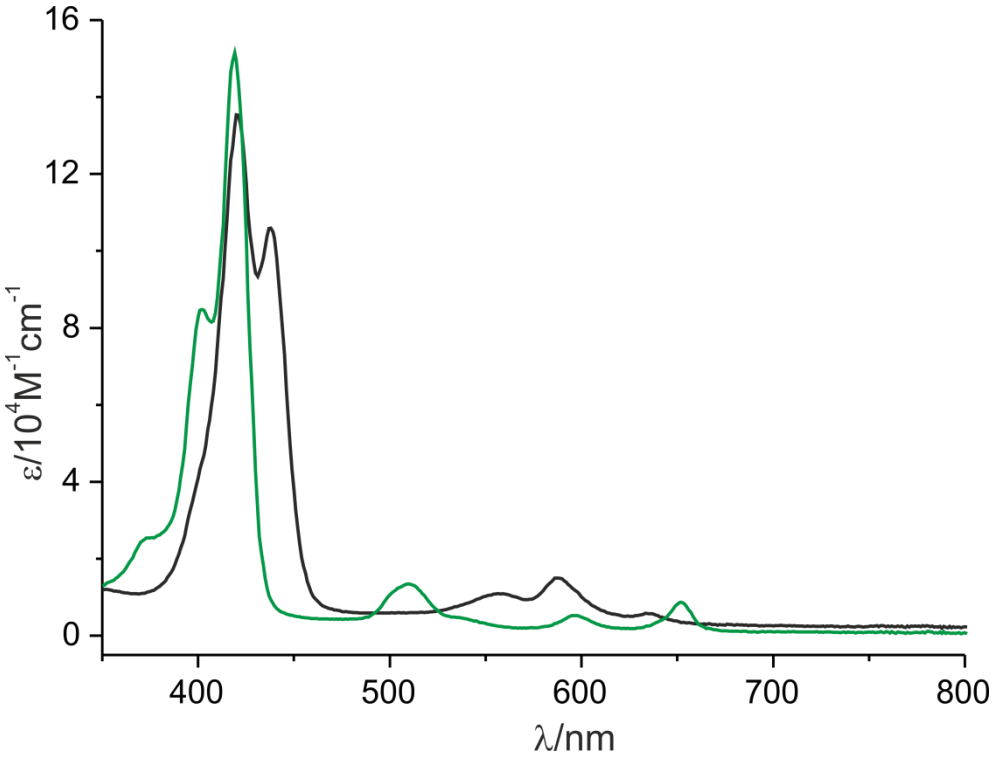

Fig. S19 The electronic absorption spectra (CH_2Cl_2) of **16** (green line) and **16-H⁺** (black line).

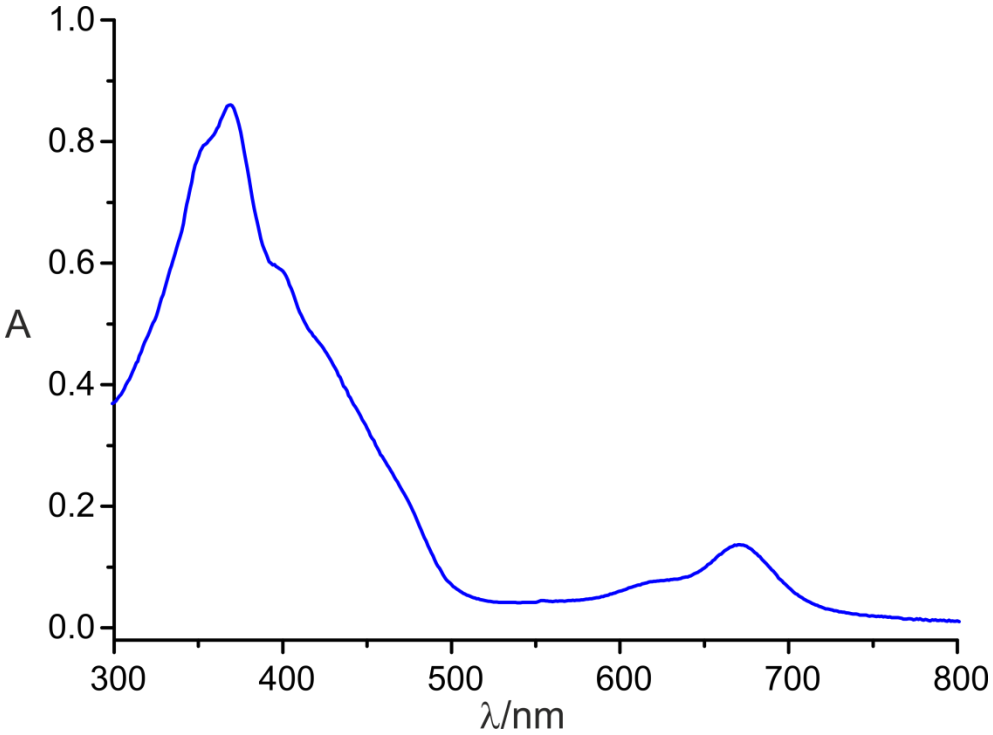

Fig. S20 The electronic absorption spectrum (CH_2Cl_2) of **17**.

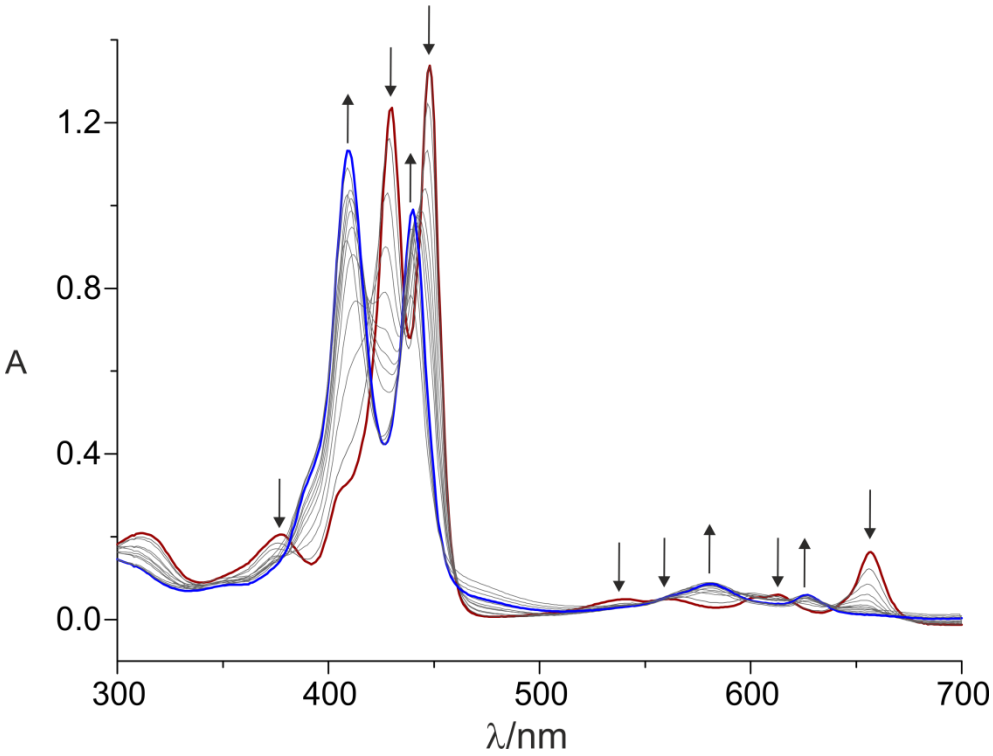

Fig. S21 Titration of **18** with TFA (CH_2Cl_2): **18** (red) and **18-H$^+$** (blue).

DFT figures and tables

Table S2. ^{1}H and ^{13}C NMR (selected) chemical shifts calculated for **17** using the GIAO method.

Position	^{1}H NMR		^{13}C NMR	
	δ_{exp}(ppm) 300 K	δ_{calc}(ppm)[a]	δ_{exp}(ppm) 300 K	δ_{calc}(ppm)[a]
5,20	6.38	5.43	121.4	116.8
12,13	6.42	6.09	128.4	122.9
7,18	6.61	6.21	122.0	116.2
8,17	5.93	5.71	118.8	114.8
***o*-Tol**	7.29	7.31, 7.44 (7.37)	132.2	128.0, 127.9 (127.9)
***m*-Tol**	7.20	7.22, 7.28 (7.25)	129.2	123.3, 123.3 (123.3)
2,3	5.31	4.17	129.5	126.2
NH	13.34	15.07	-	-
***p*-CH_3**	2.40	2.02, 2.27, 2.55 (2.28)	21.3	22.2
21	-	-	195.5	189.3

[a] The average values of calculated chemical shifts are included in brackets.

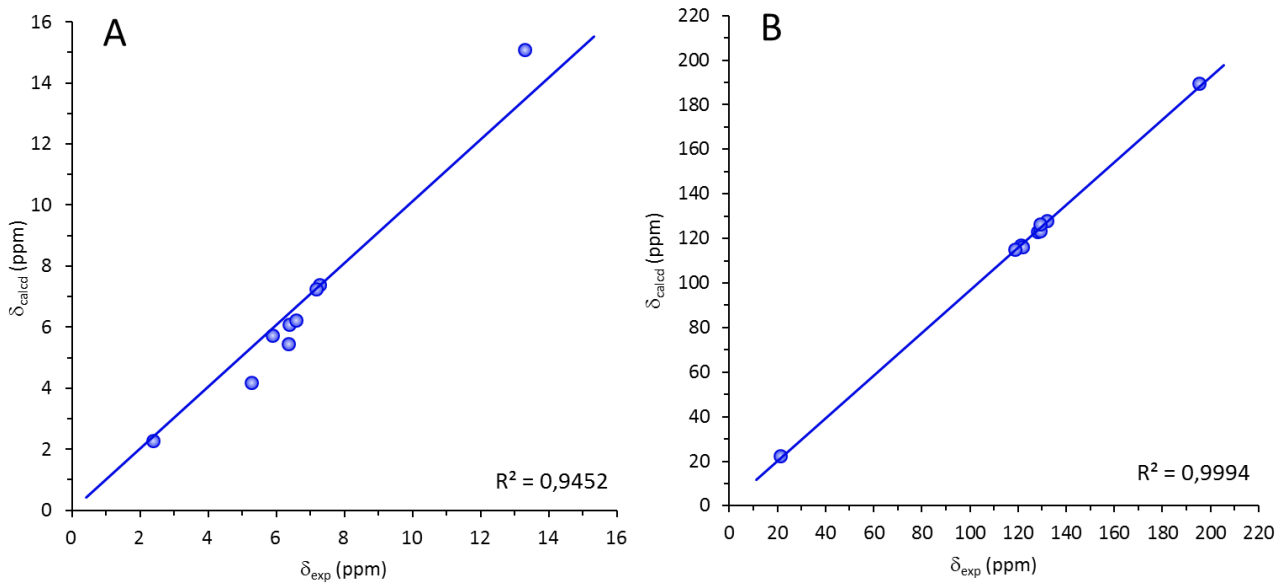

Fig. S22 Linear correlation between calculated (average values were used) and experimental values of ^{1}H (A) and ^{13}C (B) chemical shifts for **17**

Table S3. ^{1}H and ^{13}C NMR (selected) chemical shifts calculated for **18** using the GIAO method.

Position	^{1}H NMR		^{13}C NMR	
	δ_{exp}(ppm) 300 K	δ_{calc}(ppm)[a]	δ_{exp}(ppm) 300 K	δ_{calc}(ppm)[a]
5,20	9.29	9.37	118.2	114.7
12,13	8.65	8.76	125.6	120.0
7,18	8.50	8.33	121.9	116.5
8,17	8.03	8.09	122.2	117.7
***o*-Tol**	7.99	8.11, 8.29 (8.2)	133.9	131.8, 130.5 (131.1)
***m*-Tol**	7.56	7.72, 7.64 (7.68)	128.3	123.1, 123.2 (123.1)
2,3	4.53	4.63, 4.16 (4.40)	30.6	32.2
NH	2.91	1.8	-	-
***p*-CH_3**	2.67	2.5, 2.85, 2.36 (2.57)	21.5	22.4
1,4	-	-	136.9	134.2
11,14	-	-	152.1	147.6
21	-	-	179.1	167.7

[a] The average values of calculated chemical shifts are included in brackets.

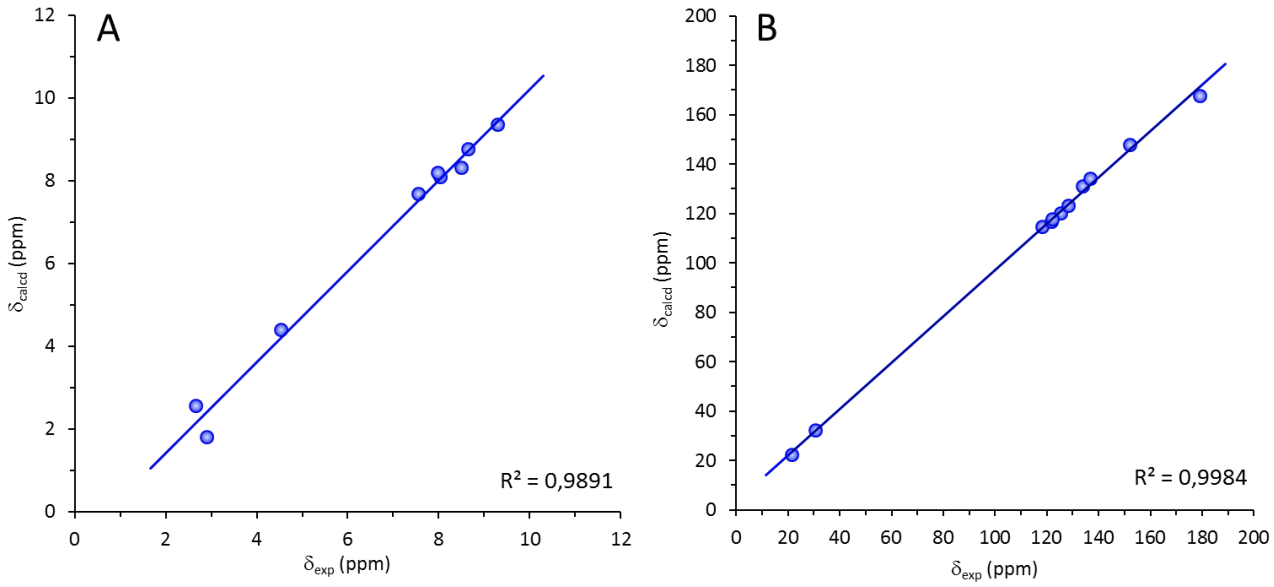

Fig. S23 Linear correlation between calculated (average values were used) and experimental values of ^{1}H (A) and ^{13}C (B) chemical shifts for **18**.

References

1. M. J. T. Frisch, G. W. Trucks, H. B. Schlegel, G. E. Scuseria, M. A. Robb, J. R. Cheeseman, G. Scalmani, V. Barone, B. Mennucci, G. A. Petersson, H. Nakatsuji, M. Caricato, X. Li, H. P. Hratchian, A. F. Izmaylov, J. Bloino, G. Zheng, J. L. Sonnenberg, M. Hada, M. Ehara, K. Toyota, R. Fukuda, J. Hasegawa, M. Ishida, T. Nakajima, Y. Honda, O. Kitao, H. Nakai, T. Vreven, J. A. Mongomery, Jr., J. E. Peralta, F. Ogliaro, M. Bearpark, J. J. Heyd, E. Brothers, K. N. Kudin, V. N. Staroverov, R. Kobayashi, J. Normand, K. Raghavachari, A. Rendell, J. C. Burant, S. S. Iyengar, J. Tomasi, M. Cossi, N. Rega, N. J. Millam, M. Klene, J. E. Knox, J. B. Cross, V. Bakken, C. Adamo, J. Jaramillo, R. Gomperts, R. E. Stratmann, O. Yazyev, A. J. Austin, R. Cammi, C. Pomelli, J. W. Ochterski, R. L. Martin, K. Morokuma, V. G. Zakrzewski, G. A. Voth, P. Salvador, J. J. Danneneberg, S. Dapprich, A. D. Daniels, Ö. Farkas, J. B. Foresman, J. V. Ortiz, J. Cioslowski, D. J. Fox, *Gaussian 09*, Revision D.01; Gaussian, Inc.: Wallingford CT, **2009**.
2. C. Lee, W. Yang, R. G. Parr, Development of the Colle-Salvetti correlation-energy formula into a functional of the electron density, *Phys. Rev. B* 1988, **37**, 785–789.
3. A. D. Becke, Density-functional exchange-energy approximation with correct asymptotic behavior, *Phys. Rev. A* 1988, **38**, 3098–3100.
4. Z. Chen, C. S. Wannere, C. Corminboeuf, R. Puchta, P. v. R. Schleyer, Nucleus-Independent Chemical Shifts (NICS) as an Aromaticity Criterion, *Chem. Rev.* 2005, **105**, 3842–3888.
5. D.Geuenich, K. Hess, F. Köhler, R. Herges, Anisotropy of the Induced Current Density (ACID), a General Method To Quantify and Visualize Electronic Delocalization, *Chem. Rev*., 2005, **105**, 7758–3772.
6. Rigaku Oxford Diffraction, *CrysAlisPRO* Software system, version 1.171.39.46, Rigaku Corporation, Oxford, UK, 2018, 2020.
7. G.M. Sheldrick, SHELXT-Integrated Space-Group and Crystal-Structure Determination, *Acta Crystallogr., Sect. A*, 2015, **A71**, 3–8.
8. G.M. Sheldrick, Crystal structure refinement with SHELXL, *Acta Crystallogr., Sect. C*, 2015, **C71**, 3–8.
9. A. L. Spek, PLATON SQUEEZE: a tool for the calculation of the disordered solvent contribution to the calculated structure factors, *Acta Crystallogr., Sect. C*, 2015, **71**, 9–18.
10. A. L. Spek, Structure validation in chemical crystallography, *Acta Crystallogr., Sect. D,* 2009, **65**, 148–155.
11. W. S. Seo, Y. J. Cho, S. C. Yoon, J. T. Park, Y. Park, Synthesis and structure of ansa-cyclopentadienyl pyrrolyl titanium complexes: [(η^5-C_5H_4)CH_2(2-C_4H_3N)]Ti(NMe_2)$_2$ and [1,3-{CH_2($_2$-C_4H_3N)}$_2$(η^5-C_5H_3)]Ti(NMe_2), *J. Organomet. Chem.,* 2001, **640**, 79–84.
12. Ulman, A., Manassen, J., Synthesis of Tetraphenylporphyrin Molecules containing Heteroatoms other than Nitrogen. Part 4. Symmetrically and Unsymmetrically Substituted Tetraphenyl-21,23-dithiaporphyrins, *J. Chem. Soc., Perkin Trans.* 1979, **1**, 1066–1069.